



Fluid Flow and Heat Transfer Simulations of the Cooling System in Low Pressure Die Casting

S. Fatih Kırmızıgöl^{1,2}, Onur Özaydın^{1*}, Sercan Acarer², Elvan Armakan¹

¹Cevher Wheels /R&D Department, İzmir, TURKEY

²İzmir Katip Çelebi University/Mechanical Engineering Department, İzmir, TURKEY

*oozaydin@cevherwheels.com

*Orcid: 0000-0001-6395-7553

Received: 01 November 2019

Accepted: 10 June 2020

DOI: Doi: 10.18466/cbayarfbe.641177

Abstract

Low pressure die casting (LPDC) is the preferred method to manufacture cost-effective automotive wheels. Cooling systems and channels of a low pressure die casting are critical to obtain better mechanical properties. Both steady-state and time-dependent (transient) Computational Fluid Dynamics (CFD) analyses of the cooling channels and the die cooling system, both in conjugate and solid-only models, are performed and the pipe flow part of the results are compared with the available experimental data. Pipes operate at a schedule transiently, therefore a complex time-dependent simulation is required. The aim is to construct a simplified approach in which only the solids (die and cast wheel) are considered and pipe cooling is represented by heat transfer coefficient distribution obtained from the much faster steady-state simulations. Successful results are obtained by significantly reducing the computational time while retaining a similar level of accuracy. Finally, cooling channels with eight different diameter stream-wise distributions are analyzed to explore their impact on pipe exit velocity and mass flow rate as a guidance towards future works. Wheels are cast with the simulated cooling system and are approved by mechanical tests.

Keywords: CFD, conjugate heat transfer, cooling channels, mass flow rate, simulation.

1. Introduction

In automotive industry, aluminum alloys are widely used because of their good mechanical strength and low weight. Lightweight aluminum castings reduce the emission values and energy consumption [1] [2]. High pressure die casting, gravity die casting and low pressure die casting (LPDC) are among the most used methods in the manufacturing of alloy wheels. LPDC utilizes Pascal's pressure theory and is a preferred process for production of components with complex shapes like wheels and engine blocks due to its advantages in turbulence-free filling and heat treatability of material used [3] [4] [5]. The well-known Pascal's theory states that a pressure change at any point in a confined incompressible fluid is transmitted throughout the fluid such that the same pressure change occurs everywhere in the confinement. Hence, pressure is essential to move the molten fluid in upward direction. LPDC molds consist of a bottom die, top die, usually four side dies, a runner and cooling channels as shown in Figure 1. Cooling channels are positioned within the top and bottom dies. There are two steps in

LPDC method. The first one is the filling process and second is the solidification process. The molten aluminum is pressurized through the runner into the wheel cavity during filling. The molten metal is then solidified via air blown onto the inner side of the mold throughout the cooling channels. The geometry and performance of the cooling channels affect the casting quality and mechanical properties of the wheel.

The cooling applied during die casting is still an immature topic and requires high technical knowledge [6] and recent studies are being carried out. As an example, Shahane et al. [7] considered modeling of solidification by numerical simulations and machine learning algorithms. The solidified metal properties are improved by optimizing water cooling locations. Neural Networks are employed to create a response surface for the finite volume solver while Genetic Algorithm is employed to optimize cooling locations. Patnaik Et al. [8] presented a similar study for the solidification in a crankcase die casting. Both line and spot cooling (with water) were considered, and it was concluded that spot cooling (impingement cooling at critical regions [9] [10]

[11]) seem to offer a better alternative relative to line cooling, which is cooling with a closed loop cooling without impingement. Another work by Hu et al. [12] is among limited studies who conducted experiments for water cooling of die casting scenario. They presented the high amount of heat removal, especially at the beginning of cooling cycle. Mehr et al. [13] recently had similar observations.

Eck et al. [14] conducted experiments for natural convection with water, which may induce a softer cooling relative to forced convection and thus may reduce thermal stresses [15] [16] [17] [18]. Cells inside the molts are filled with continuously cooled water. The stationary water applies cooling by natural convection. The temperature field is obtained as the main findings of this study.

In order to reduce thermal shocks during solidification of the molted metals, spraying lubricants is a promising method. Liu et al. [19] were among the pioneers to conduct specific experiments on water spray cooling applicable to die casting. They provided a comprehensive correlation of heat transfer coefficient as a function of droplet properties such as droplet diameter, velocity, etc. In another study on spray cooling of die casting, Sabau and Wu [20] have shown that even spray cooling creates significant thermal shocks during the initial stages of the spray.

Air cooling is a viable alternative for controlled cooling of molted metal with softer cooling effect [21]. However, the topic is not mature and studies are highly limited in this area. This study considers air cooled LPDC as the solution to eliminate thermal shocks by lower but more steady cooling rates. Cooling channels are positioned on the top and bottom dies and air is used as the cooling fluid (Figure 1). A certain amount of air passes in the cooling channels according to the pipe diameter and supply pressure. Computational Fluid Dynamics (CFD) simulations are utilized to model current cooling channels and the mass flow rate passing through it is obtained. With a parametric study, inlet and outlet pipe diameters of the cooling channel system is changed to achieve the maximum cooling velocity while also reducing or keeping constant the mass flow rate.

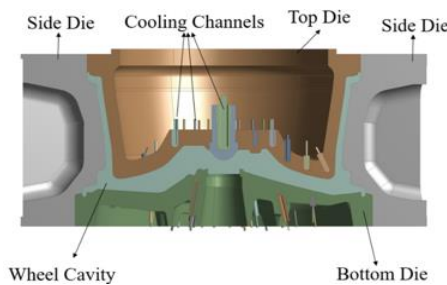


Figure 1. Schematic of LPDC's components (redrawn from [22]).

2. Numerical Simulations

The existing cooling channels have 4 mm outlet (jet) pipe diameter and 8 mm inlet (connection) diameter. The mid diameter is 12 mm as shown in Figure 2. ANSYS Fluent, a commercial cell-centered finite volume method solver is used for the CFD analyses. It is a commonly used and established software, employed for various purposes related to fluid dynamics [23] [24] [25].

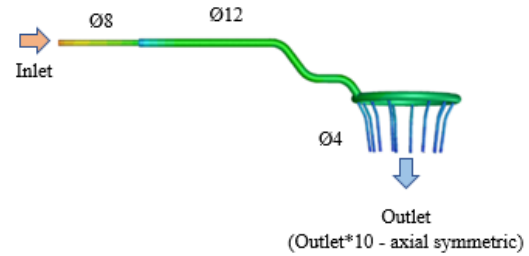


Figure 2. A sample pipe network of the existing cooling channel system (color is for wall pressure).

2.1. Turbulence Closure Model Selection

The turbulence models built-in in the code such as k-ε realizable, k-ω, transition k-kl-ω, transition SST, Spalart-Allmaras are compared with respect to experimental results obtained in-house. Cooling channels are analyzed with each of these turbulence models to examine the accuracy of the CFD simulations.

Total pressure (P_t) at the pipe inlet is measured with a manometer; and density, mass flow rate, volumetric flow rate and velocity of the air are calculated by using equations (1), (2), (3), (4), (5) and assuming the pipe exit static pressure (P_s) is atmospheric:

$$\frac{P_s}{P_t} = \left(1 + \frac{\gamma-1}{2} M^2\right)^{\frac{\gamma}{\gamma-1}} \quad (2.1)$$

$$M = \frac{V}{a} \quad (2.2)$$

$$a = \sqrt{\gamma R T_s} \quad (2.3)$$

$$\dot{m} = \rho V A \quad (2.4)$$

$$\dot{V} = V A \quad (2.5)$$

Table 1. Accuracy of turbulence model w.r.t experimental data

	Transition SST	Transition k-kl-ω	k-ω SST	k-ε Realizable	k-ε RNG	Spalart Allmaras	Exp. Data
P_t [Pa]	472.2	472.2	472.2	472.2	472.2	472.2	472
P_s [Pa]	388.3	386.6	388.0	390.0	390.6	390.5	390
ρ [kg/m ³]	4.76	4.75	4.76	4.78	4.78	4.78	4.78
\dot{m} [kg/s]	0.0427	0.0431	0.0428	0.0424	0.0423	0.0423	0.0430
\dot{V} [m ³ /s]	0.00896	0.00906	0.00898	0.00886	0.00883	0.00884	0.00899
u [m/s]	181	182.9	181.3	179.0	178.3	178.5	178.9

Table 1 compares different turbulence models with respect to experimental data. Here, P_t and P_s refer to total and static pressure, respectively. ρ is density and m is mass flow rate. V is volumetric flow rate and u is velocity. and it has been found that k- ϵ realizable model has the best correlation. Therefore, the k- ϵ realizable model is chosen.

2.2. Conjugate Heat Transfer CFD Analyses of LPDC System

This section discusses conjugate heat transfer (CHT) simulations of the die cooling system, where the temperature distribution on the dies is the main parameter of interest. The exit portions of the cooling pipe system are taken as the mass flow inlet for the conjugate die cooling scheme presented in Figure 3. Since only the exit portions of the cooling pipes are taken, the length of these are determined to maintain fully developed flow at the jet (outlet) location. Flow exit for the CFD are taken as the exits of cooling pockets, where an almost atmospheric pressure exists since there is no significant blockage prior to mixing with external atmosphere. Transient Reynolds averaged Navier-Stokes equations (RANS) for ideal-gas compressible air are discretized by finite volume method with second order upwind scheme for all parameters and second order implicit accuracy in time advancement [26].

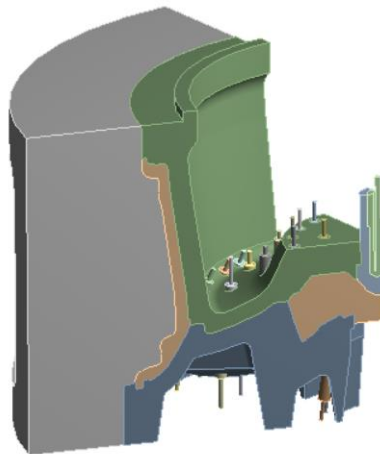


Figure 3. Geometry of die in LPDC system.

The mesh independency study was conducted in the cooling channels which are critical parts for the heat transfer and occurred impingement flow region in there. The different number of elements generated by changing body and face sizes and at constant mass flow rate how the mesh quality affects CFD simulation results. 720.000 number of elements chosen for one cooling channel in Figure 4. The error percentage is less than 1 both heat flux and velocity due to 2.5 M elements. Temperature (700K) has been defined to the wall of the cooling channels to compare heat fluxes.

The conjugate heat transfer (CHT) allows the combined simulation of fluid and solid domains. Since pipes operate on a schedule transiently so the cooling channels operate for different periods, a transient analysis is required. A simplified approach is to only model solids, in which computational time can greatly reduce. In this case, heat transfer coefficient detailed profiles must be given in the impingement locations, which is the main difficulty. The mesh structure is created according to mesh independency study for the cooling channels and solid parts or dies are structured due to the fluid mesh structure as shown in Figure 5. A periodic model is considered due to geometrical periodicity.

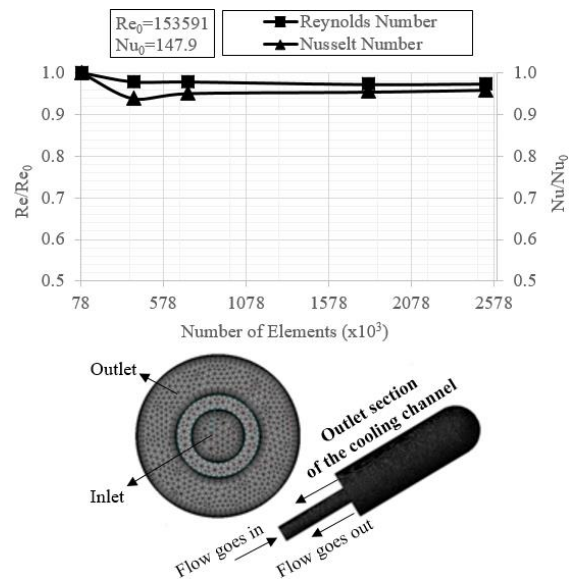


Figure 4. Mesh independency study.

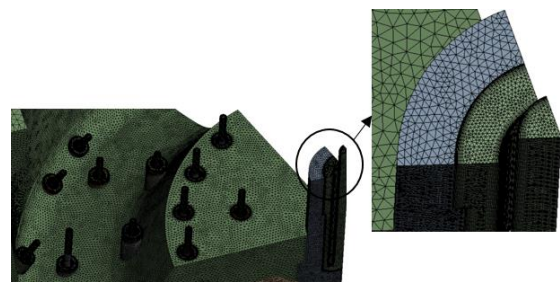


Figure 5. Mesh structure of die and outlets of the cooling channels.

Figure 6 presents Mach number field in the cooling jets at an instant. The jet profiles are variable due to variable mass flow rate and pressure entering each cooling hole. Supersonic flow is obviously seen towards the exit of the jets, where overexpansion after the exit of the jet causes Mach numbers as high as 1.6. This flow regime changes with time based on the cooling schedule being applied. However, time dependent solution of the complete process is solved for the detailed conjugate

heat transfer approach. Figure 7 presents the corresponding Nusselt number field at the cooling holes at the same instant. Here, the reference length used in the Nusselt number is taken as the diameter of the cooling holes. The reference temperature is taken as the coolant inlet temperature. As expected, the impingement locations have the highest Nusselt numbers, and the Nusselt numbers reduces towards the outlets of the cooling holes. Some holes have zero Nusselt number, which indicates these local cooling mass flow rates are zero based on the cooling schedule.

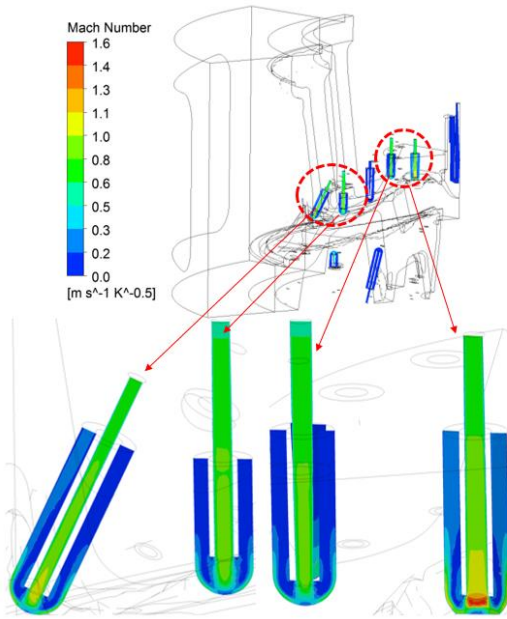


Figure 6. Cooling jet Mach number profiles.

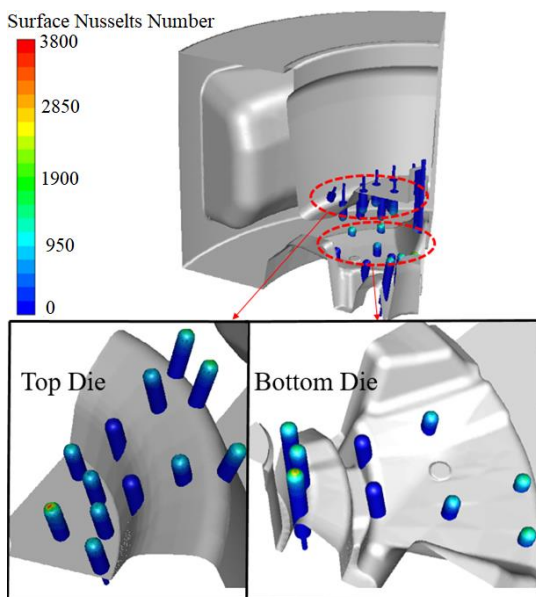


Figure 7. Nusselt Number distribution at the cooling holes.

Figure 8 presents the variation of area weighted Nusselt number in the cooling hole as a function of coolant entry Reynolds number. The expected steep rise is obtained by the CFD simulations. Here, the nominal Reynolds number, which is realized when the nominal setting of the supply air compressor is selected (6 bars supply pressure).

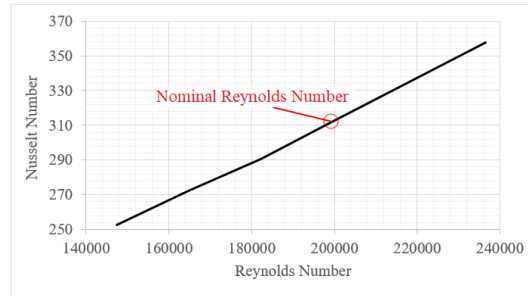


Figure 8. The simulated function of area weighted average Nusselts number as a function of coolant entry Reynolds number.

For the simplified second alternative, heat transfer coefficient distributions are obtained from steady state full CHT analyses, disregarding the transient schedule and assuming all the pipes simultaneously operate, therefore analyses with much lower computational cost can be done this way. The obtained heat transfer coefficient distributions (which are similar to the ones presented in Figure 7, but the steady versions of them) are then specified in the solid-only model. The results for the both cases are presented in Figure 9 (a) and Figure 9 (b), respectively as a section.

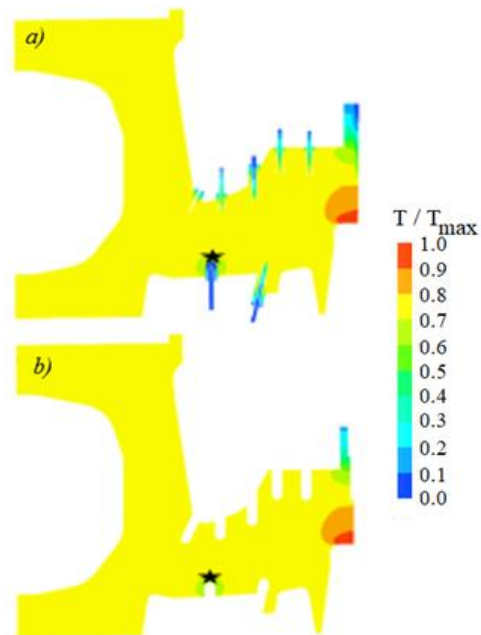


Figure 9. A section plane from 3D Conjugate Heat Transfer Analysis with time dependent solution.

The results are compared and there is no significant difference in temperature distributions. A probe point is placed inside the solid, close to coolant impingement region of one of the cooling pockets as shown in Figure 9 by a star. Time evolution of temperature at this point is also observed for the two approaches, which are presented in Figure 10. It is evident that the temperature distributions are the same for the two approaches. In the figures, the temperature scale is taken between 0-1 to represent a scale in between the minimum and maximum temperatures, respectively.

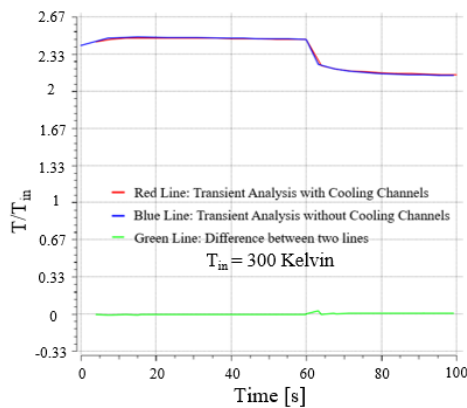


Figure 10. Temperature time evolution at the probe point.

2.3. Parametric Analysis of the Cooling Channels

Once the conjugate heat transfer analyses with the existing pipe configuration is carried out, the cooling

Table 2. Results for the cooling channel CFD simulations.

Design No.	Cooling Channels Geometry	Mass Flow Rate (m ³ /s) x100	Inlet Velocity (m/s)	Avg. Outlet Velocity (m/s)
Reference (Existing)	Ø8-Ø12-Ø4	6.26	226.89	334.87
1	Ø8-Ø12-Ø3	5.44	181.51	352.15
2	Ø8-Ø12-Ø2	2.96	88.45	356.64
3	Ø10-Ø12-Ø4	9.02	198.02	351.18
4	Ø10-Ø12-Ø3	6.38	126.49	356.20
5	Ø10-Ø12-Ø2	3.03	56.93	355.97
6	Ø12-Ø12-Ø4	10.00	139.89	352.49
7	Ø12-Ø12-Ø3	6.40	84.97	354.04
8	Ø12-Ø12-Ø2	2.83	39.56	356.99

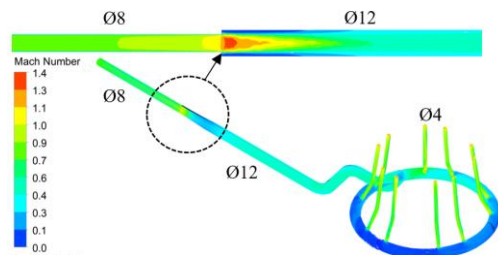


Figure 11. Mach number distribution for the original geometry.

pipe system is considered to explore sensitivity of the mass flow rate and jet velocities as a function of pipe diameter distribution. Inlet and outlet diameters are parameterized as ϕ_1 and ϕ_3 while the connecting pipe diameter in between the inlet and outlet (ϕ_2) is kept fixed.

Those are presented in Figure 2. The inlet diameter is varied in 3 levels as Ø8-Ø10-Ø12 mm and outlet diameter is varied in 3 levels as Ø2-Ø3-Ø4 mm.

Eight different configurations presented in Table 2 are analyzed in addition to the original (existing) design. Design No. 2 and 8 are the best-performing geometries in terms of minimal mass flow rate and inlet velocity, and maximal outlet velocity. Cooling channel is produced with accordance to design no 2 and the cast wheel had been verified by mechanical tests. The analyses show that even if the mass flow rate is reduced inside the channel, aluminum wheel can be produced without any casting problems.

Figure 11 presents the Mach distribution in the existing reference geometry of cooling piping system originally presented in Figure 2. Figure 12 presents the design no 2 results for the Mach number distribution. According to CFD analysis results, the inlet Mach (and hence the velocity) is decreased as shown by the blue region in Figure 12 relative to the yellow region in Figure 11. Outlet velocity is increased as shown in Table 2.

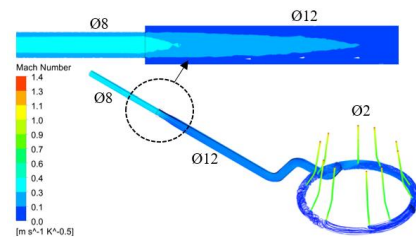


Figure 12. Mach number distribution for the cooling channel design no 2.

Flow separation is encountered in reference geometry as shown in Figure 11. This flow separation causes turbulent flow and additional pressure losses, resulting in a decreased exit jet velocity. On the other hand, the flow in the design no. 2 and design no 8 shown in Figure 12 and Figure 13 has much lower mass flow rate and favorable flow characteristics. Thus, due to reduced pipe diameter and losses, there is an increase in the velocity at the outlet. Design no 2 is selected as the modified (future) design, which is verified in another published work of the same research team [27].

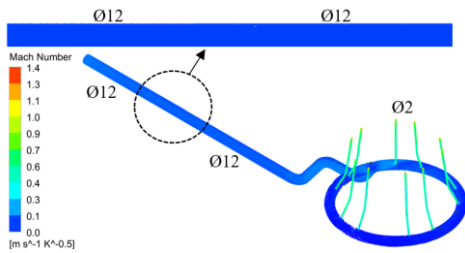


Figure 13. Mach number distribution for the cooling channel design no 8.

Pressure drop also occurs in the elbow as shown in Figure 14, which results in a decreasing mechanical energy along the pipe. This effect can occur to prevent the best cooling performance and cause abrupt change in velocity and pressure as shown in Figure 15. Sudden accelerations and subsequent sudden decelerations and flow separation zone can be identified in Figure 15. However, the elbow is kept unaltered due to field requirements.

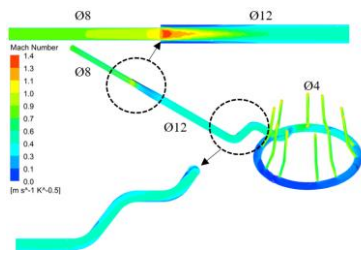


Figure 14. Elbow of the in-use geometry.

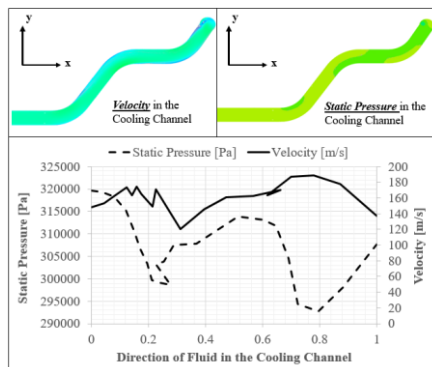


Figure 15. Changing of velocity and pressure at elbow.

Finally, the normalized (percent the inlet total pressure) and physical total pressure losses of the final pipe system (design no:2 in Table 2) is presented in Figure 16. The variation of Reynolds number is established by altering the inlet total pressure. As expected, the increasing Reynolds number causes slightly less relative pressure losses. This is because viscous effects become relatively weaker and inertia effects becomes stronger (also friction factor reduces as Reynolds number increases, here CFD captured this trend). On contrary, the physical (non-normalized) pressure loss increases with Reynolds number, primarily due to increase in velocity.

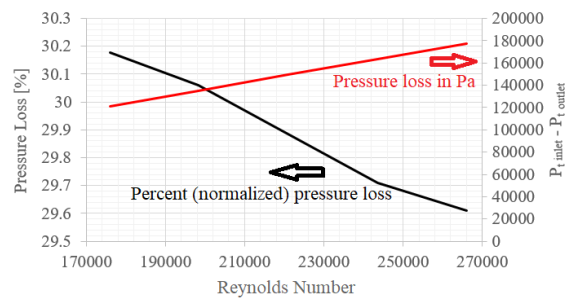


Figure 16. Normalized and physical pressure losses in design no 2.

3. Conclusions

This study describes the method to conduct a conjugate heat transfer (CHT) simulation in a die cooling system, which received very limited attention in the open literature. Initially, selecting optimal turbulence model based on pipe flow experimental data and corresponding pipe CFD analyses and the computational model is discussed. Once these are established, time consuming full CHT and the much faster simplified solid-only transient heat transfer analyses of the die cooling system are compared. These comparative studies indicate solid-only simulations taking detailed impingement heat transfer coefficient profiles from steady-state CHT analysis (much faster than the transient CHT due to the steady-state solution) as inputs had yielded to similar accuracies relative to the more time consuming fully transient CHT analyses. Therefore, even if the pipes operate on a schedule transiently, heat transfer coefficients relative to the steady state case in which all pipes operate simultaneously does not significantly change. Therefore, solid-only simulations can be performed based on the pipe cooling schedule transiently. Moreover, after the system simulations with the existing pipe system, pipe-only domain (ending at jet exit assuming atmospheric discharge pressure) is considered. Parametric investigation of stepwise diameter distribution along the flow direction has been conducted in order to obtain a design with maximum possible outlet velocity with minimum mass flow rate as a guideline towards future works. In this regard, the



pipe system design no 2 is selected as the final configuration and the wheels cast with this cooling system are approved by mechanical tests.

Acknowledgement

The authors would like to thank Cevher Wheels Company for the permission to publish this article.

Author's Contributions

S. Fatih Kırmızıgöl: Drafted and wrote the manuscript, performed the experiment and result analysis.

Onur Özaydın: Drafted and wrote the manuscript, performed the experiment and result analysis.

Sercan Acarer: Supervised the experiment's progress, result interpretation and helped in manuscript preparation.

Elvan Armakan: Supervised the experiment's progress, result interpretation and helped in manuscript preparation.

Ethics

There are no ethical issues after the publication of this manuscript.

References

- [1] J. Sun, Q. Le., L. Fu, J. Bai, J. Tretter, K. Herbold and H. Huo, "Gas Entrainment Behavior of Aluminum Alloy Engine Crankcases During the Low-Pressure-Die-Casting Process," *Journal of Materials Processing Technology*, vol. 266, pp. 274-282, 2016.
- [2] M. Ayvaz and H. Çetinel, "Farklı Alüminyum Alaşımlarının, TIG Kaynak Yöntemi ile Kaynatılması ve Mekanik Özelliklerinin İncelenmesi," *Celal Bayar University Journal of Science*, vol. 7, no. 1, pp. 39-46, 2011.
- [3] G. Timelli, D. Caliori and J. Rakhmonov, "Influence of Process Parameters and Sr Addition on the Microstructure and Casting Defects of LPDC A356 Alloy for Engine Blocks," *Journal of Materials Science and Technology*, vol. 32, no. 6, pp. 515-523, 2016.
- [4] M. Başaranel, N. Saklakoglu and S. İrizalp, "Etial 180 Alüminyum Alaşımına İlave Edilen Mg ve Sn Elementlerinin İntermetalik Fazlara Etkisi," *Celal Bayar University Journal of Science*, vol. 9, no. 2, pp. 17-23, 2013.
- [5] X. Teng, H. Mae, Y. Bai and T. Wierzbicki, "Pore Size and Fracture Ductility of Aluminum Low Pressure Die Casting," *Engineering Fracture Mechanics*, vol. 76, no. 8, pp. 983-996, 2009.
- [6] K. Seah, J. Hemanth, S. Sharma and K. Rao, "Solidification behaviour of Water-Cooled and Subzero Chilled Cast Iron," *Journal of Alloys and Compounds*, vol. 290, no. 1-2, pp. 172-180, 1999.
- [7] S. Shahane, N. Aluru, P. Ferreira, S. Kapoor and S. Vanka, "Optimization of Solidification in Die Casting Using Numerical Simulations and Machine Learning," *Journal of Manufacturing Processes*, vol. 51, pp. 130-141, 2020.
- [8] L. Patnaik, I. Saravanan and S. Kumar, "Die Casting Parameters and Simulations for Crankcase of Automobile Using MAGMASoft," *Materials Today: Proceedings*, vol. 22, no. 3, pp. 563-571, 2020.
- [9] H. Fawzy, Q. Zheng, Y. Jiang, A. Lin and N. Ahmad, "Conjugate Heat Transfer of Impingement Cooling Using Conical Nozzles with Different Schemes in a Film-Cooled Blade Leading-Edge," *Applied Thermal Engineering*, vol. 177, p. 115491, 2020.
- [10] T. Wei, H. Oprins, V. Cherman, E. Beyne and M. Baelmans, "Experimental and Numerical Investigation of Direct Liquid Jet Impinging Cooling Using 3D Printed Manifolds on Lidded and Lidless Packages for 2.5D Integrated Systems," *Applied Thermal Engineering*, vol. 164, p. 114535, 2020.
- [11] L. Chen, R. Brakmann, B. Weigand, R. Poser and Q. Yang, "Detailed Investigation of Staggered Jet Impingement Array Cooling Performance with Cubic Micro Pin Fin Roughened Target Plate," *Applied Thermal Engineering*, vol. 171, p. 115095, 2020.
- [12] H. Hu., F. Chen, X. Chen, Y. Chu and P. Cheng, "Effect of Cooling Water Flow Rates on Local Temperatures and Heat Transfer of Casting Dies," *Journal of Materials Processing Technology*, vol. 148, no. 1, pp. 57-67, 2004.
- [13] F. Mehr, S. Cockcroft, C. Reilly and D. Maijer, "Investigation of the Efficiency of a Water-Cooled Chill on Enhancing Heat Transfer at the Casting-Chill Interface in a Sand-Cast A319 Engine Block," *Journal of Materials Processing Technology*, vol. In Press, p. 116789, 2020.
- [14] S. Eck, M. Kharicha, A. Ishmurzin and A. Ludwig, "Measurement and Simulation of Temperature and Velocity Fields During the Cooling of Water in a Die Casting Model," *Materials Science and Engineering: A*, Vols. 413-414, pp. 79-84, 2005.
- [15] R. Akyüz, E. Kulalı, R. Soncu, C. Öztürk and M. Karaca, "Measuring of Core Split Line Defect on Pillar Type Vented Brake Disc and Investigation of Crack Occurrence Potential on the Disc Caused by Its Geometric Deviation," *Celal Bayar University Journal of Science*, vol. 16, no. 1, pp. 1-7, 2020.
- [16] S. Gain, T. Silva, A. Jesus, A. Cavaleiro, P. Rosa and A. Reis, "Mechanical Characterization of the AlSi9Cu3 Cast Alloy Under Distinct Stress States and Thermal Conditions," *Engineering Fracture Mechanics*, vol. 216, p. 106499, 2019.
- [17] B. Milkereit, H. Fröck, C. Schick and O. Kessler, "Continuous Cooling Precipitation Diagram of Cast Aluminium Alloy Al-7Si-0.3Mg," *Transactions of Nonferrous Metals Society of China*, vol. 24, no. 7, pp. 2025-2033, 2014.
- [18] V. Kırmacı, "Vorteks Tüpünde Akışkan Olarak Kullanılan Hava Ve Argonun Soğutma Isıtma Sıcaklık Performanslarının Deneysel Olarak İncelenmesi," *Celal Bayar University Journal of Science*, vol. 3, no. 2, pp. 191-199, 2007.
- [19] G. Liu, Y. Morsi and B. Clayton, "Characterisation of the Spray Cooling Heat Transfer Involved in a High Pressure Die Casting Process," *International Journal of Thermal Sciences*, vol. 39, no. 5, pp. 582-591, 2000.



- [20] A. Sabau and Z. Wu, "Evaluation of a Heat Flux Sensor for Spray Cooling for the Die Casting Processes," *Journal of Materials Processing Technology*, vol. 182, no. 1-3, pp. 312-318, 2007.
- [21] J. Lin, A. Mahvi, T. Kunke and S. Garimella, "Improving Air-Side Heat Transfer Performance in Air-Cooled Power Plant Condensers," *Applied Thermal Engineering*, vol. 170, p. 114913, 2020.
- [22] B. Zhang, D. Majjer and S. Cockcroft, "Development of a 3-D Thermal Model of the Low-Pressure Die-Cast (LPDC) process of A356 aluminum alloy wheels," *Materials Science and Engineering: A*, vol. 464, no. 1-2, pp. 295-305, 2007.
- [23] N. Yıldırım, J. Buchlin and C. Benocci, "Simulation of Surface Instability at the Interface of Two Fluids," *Celal Bayar University Journal of Science*, vol. 13, no. 2, pp. 365 - 377, 2017.
- [24] M. Özdoğan, B. Sungur, L. Namli, B. Topaloğlu and A. Durmuş, "A Comparative Study of Turbulence Model Effects in Numerical Analyzing Flow around the Buildings Having Various Aspect Ratios," *Celal Bayar University Journal of Science*, vol. 12, no. 3, pp. 585 - 595, 2016.
- [25] P. Sharma, L. Chandra, P. Ghoshdastidar and R. Shekhar, "A Novel Approach for Modelling Fluid Flow and Heat Transfer in an Open Volumetric Air Receiver using ANSYS-FLUENT," *Solar Energy*, vol. 204, pp. 246-255, 2020.
- [26] ANSYS Inc., "Ansys Fluent Theory Guide," 2013.
- [27] O. Özaydın, E. Armakan and Y. Çatal, "Soğutma Kanallarındaki Hava Tüketimi Azaltılması," *TÜRKDÖKÜM*, vol. 52, no. Temmuz Ağustos Eylül Sayısı, pp. 80-84, 2019.